Experimental Investigation into Electric Vehicle Battery Diversity

1st Bachir ZINE
University of Eloued-Algeria
zine-bachir@univ-eloued.dz

2nd Redha Meneceur
University of Eloued-Algeria
r.meneceur39@gmail.com

3rd Labiod Chouaib[3]
University of Eloued –Algeria
labiod-chouaib@univ-eloued.dz

4rd Mohamed BECHERIF
Femto-ST UMR CNRS 6174 - FCLab
FR CNRS 3539,
Univ.Bourgogne France-Comté/UTBM,
Belfort, France
mohamed.becherif@utbm.fr

***Abstract*— This study conducts experimental investigations into the diversity of electric vehicle (EV) batteries, employing a comparative approach. The primary focus is on analyzing the performance of two distinct battery types under varying states of charge (SOC), utilizing the coulomb counting method. Additionally, a generic battery model is employed to facilitate the comparison process. The experimental setup aims to provide valuable insights into the behavior and characteristics of different EV batteries, contributing to the enhancement of battery technologies for future electric vehicle applications.**

Keywords— Experimental Investigations, Electric Vehicle Batteries, Battery Diversity, Comparative Analysis, State of Charge (SOC), Coulomb Counting Method, Generic Battery Model.

I. INTRDUCTION

Recently, electric vehicles have gained enormous popularity due to their performance and efficiency. The investment in developing this new technology is justified by the increased awareness of the environmental impacts caused by combustion vehicles, such as greenhouse gas emissions, which have contributed to global warming and the depletion of oil reserves that are not renewable energy sources.

Battery Management Systems (BMS) must be able to provide an accurate real-time estimate for the Battery State of Charge (SOC) and State of Health (SOH). The SOC value is so critical information for the BMS especially if the battery is the only source of power and the system is not connected to the network. Since the SOC is not directly measurable or captured, it causes the main challenge of finding and proposing different estimation methods.

The literature introduces different approaches for estimating the SOC, this review divides the SOC estimation methods into five categories, which are shown in Figure 1.[1].

In conventional methods, SoC estimation occurs indirectly by combining the physical characteristics of the battery, such as voltage, current, resistance, temperature, and impedance [1-14].

Methods Based on Filtering Algorithms [15-63], Methods Based on Nonlinear Observers [64-68], Methods Based on Learning Algorithms [69-95], Hybrid Methods [96-102].

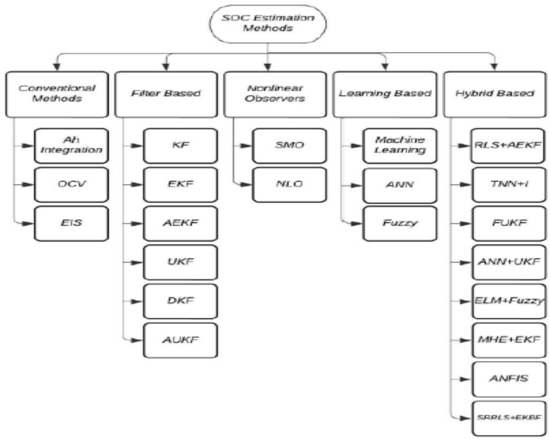

Fig.1. Classification of SOC estimation methods [1]

Table.1 sums up the benefits and drawbacks of four SOC assessment strategies just as their exhibitions in exactness and strength.

TABLE I. COMPARATIVE ANALYSIS OF THE SOC METHODS

Methodology	Method	Main Results	Advantages	Disadvantages	Considerations and Limitations
conventional methods	**Ah OCV EIS**	**Those that show error values have an RMSE of 1.65% which is a hybrid model with machine learning**	**No need for an algorithm to implement**	**Battery needed to be in resting mode for long time**	**Authors who did not present errors performed simulations or measurement tests. The hybrid algorithm obtained results from physical tests with an embedded algorithm**
Methods Based on Filtering Algorithms	**KF EKF AKF UKF DKF AUKF**	**MAE-range of values 0.0426% to 2.22%, RMSE-range of values 0.0044% to 4.58%; these vary depending on the filter used**	**Acceptable accuracy, dealing with white noise**	**Need for an accurate enough battery model, extensive time and computational memory, and a complicated algorithm to implement**	**The method's accuracy is linked to the accuracy of the battery model. Such processes need longer execution time and memory because they have a more complex algorithm**

Methods Based on Nonlinear Observers	**SMO NLO**	**MAE-0.928% RMSE-1.7%**	**Acceptable accuracy and robustness against modeling uncertainties**	**Difficult for online application due to the complicated computational algorithm**	**The authors performed physical tests. Still, nonlinear methods are difficult to apply online due to the algorithm's complexity**
Methods Based on Learning Algorithms	**Technique of machine and deep learning, ANN and their variations, fuzzy logic**	**MAE-range of values 0.001929 % to 3%, RMSE-range of values 0.018% to 3%**	**Powerful ability to approximate nonlinear functions**	**Need for a large number of data to train the algorithm applicable for all operating conditions**	**Applicable for all operating conditions but need a large number of data for algorithm training; they also require more processing time and cost**
Hybrid Methods	**RLS + AEKF, TNN + I, FUKF, ANN+UKF, ELM+Fuzzy, MHE+EKF, ANFIS, SRRLS+EKBF**	**RMSE-range of values 0.01119 % to 3%; these vary depending on the filter used**	**They reduce the cost of the system but also make the estimation results more effective and reliable**	**Combining two or three methods is a laborious task and has high complex computation**	**The combination of the two strategies increases the accuracy of the system**

The goal of this work is to compare two different batteries capacities through empirical measurements of battery voltage and current using the Ampere-hour integral estimation method with constant and variable C-rates of discharge current.

II. AMPERE HOUR METHOD

Coulomb Counting method ((known as the current integration method) is chosen and is considered to be the most commonly used to estimate the SOC. It consists of measuring the battery open circuit voltage at start-up to estimate the initial SOC using the battery datasheet information. Then, the battery current is integrated to estimate the amount of charge delivered (or recovered given a charge) by the batteries. This is based on the concept of SOC, as seen in Eq.1, where knowledge of the initial SOC is therefore needed to determine the state of charge [103] [104] [105]. Based on this approach, the SOC for the battery estimate is calculated as follows [106]:

$$\mathbf{SOC=SOC_0} - \frac{1}{C_N}\int_{t0}^{t} \eta . I(\tau)\, d\tau \qquad \textbf{(1)}$$

If the initial value of the charge state SOC_0 is specified, or imposed (technically, most researcher imposes the initial state as to be fully charged or fully discharged), the method of coulomb counting becomes very precise and especially simple to determine the SOC [107]. But this method is less accurate if the SOC_0 is unknown.

The coulomb counting strategy computes the remaining stored energy essentially by collecting the charge moved in or out of the battery. The precision of this strategy depends fundamentally from a real estimation of the battery current and precise assessment of the initial SOC. With a pre-knowledge of the initial SOC, which also can be stored at the end of the vehicle trip in a flash memory to be reused as the initial SOC for the next trip (and neglecting the battery self-discharge), the battery SOC can be determined by computing the stored and the released energy flows over the operating time [108]. Nevertheless, the stored energy in the battery is not completely available to be used due to the DOD (Depth of Discharge) which is a quantity of energy to keep inside the battery to avoid its damaging. As a consequence, there are losses during charging and discharging. For more exact SOC assessment, these effect should be considered [109]. Also, the SOC must be recalibrated consistently and discharge limit should be considered for more exact assessment.

III. GENERIC BATTERY MODEL

The battery model can be obtained by considering a voltage source in series with constant resistance, as appeared in Equation.2. [110]

$$V_{batt} = \mathbf{E_0 - K}\frac{Q}{Q-i_t}\cdot i_t - \mathbf{R{\cdot}I + A.exp\ (\text{-}B}\cdot i_t) K\frac{Q}{Q-i_t}\cdot i^* \qquad \textbf{(2)}$$

The special feature of this model is the use of filtered current (i*) through the polarization resistance. This filtered current solves the problem of the algebraic loop due to the simulation of power systems in Simulink.[111].

Although the existence of an hysteresis between the charging and discharging of the battery voltage, this model is still valid for both charge and discharge cycles [112]. The open voltage source is determined with a non-straight condition dependent on the battery genuine SOC.

The battery models can be obtained using:

- ✓ The charge model ($i^*<0$)

$$f_1(it, i^*, exp, batt\ type) = \mathbf{E_0\text{-}\ K.}\frac{Q}{i_t - 0.1Q}\mathbf{.\ i^*\ \text{-}\ K.}\frac{Q}{i_t - Q}\mathbf{.}i_t \mathbf{\ +\ Exp(t)} \quad \textbf{(3)}$$

- ✓ The discharge model ($i^*>0$)

$$f_1(it, i^*, exp, batt\ type) = \mathbf{E_0\text{-}\ K.}\frac{Q}{i_t - Q}\mathbf{.\ i^*\ \text{-}\ K.}\frac{Q}{i_t - Q}\mathbf{.}i_t \mathbf{\ +\ Exp(t)} \quad \textbf{(4)}$$

This model is based on assumptions and has its limitations.

A. Application

- ✓ 1ST BATTERY

From the discharge curve provided by the manufacturer, the parameters are extracted in Table.2

TABLE II. 1ST BATTERY PARAMETERS

Nominal voltage(V)	12
Rated capacity(Ah)	100
Initial State of charge (%)	100
Maximum capacity(Ah)	110
Fully charged voltage (V)	12.72
Nominal discharge current(A)	10
Internal resistance (ohms)	0.0057
Capacity(Ah)@nominal voltage	59.37
Exponential zone [voltage(V), capacity (Ah)]	[12.48, 10]

- ✓ 2ND BATTERY

From the discharge curve provided by the manufacturer, the parameters are extracted in Table.3.

TABLE III. 2ND BATTERY PARAMETERS AT C-RATES OF DISCHARGE

C-rates of discharge	0.25C	0.17C	0.09C	different C rates
Nominal Voltage (V)	12	12	12	12
Rated Capacity (Ah)	52	52	52	52
Initial State of Charge (%)	100	100	100	100
Maximum Capacity (Ah)	40.1999	53.8	47.5	47.5
Fully Charged Voltage (V)	12.7	12.8	12.9	12.9
Nominal Discharge Current (A)	13	8.84	4.68	12
Internal Resistance (ohms)	0.0055	0.0055	0.0055	0.0055
Capacity (Ah) @ Nominal Voltage	38.2	44.80	46	46
Exponential Zone (Voltage(V), Capacity (Ah))	[12.7 2.5]	[12.8 1.9]	[12.9 2.225]	[12.9 2.225]

III. EXPERIMENTAL METHOD

A. *Battery specification*

✓ 1ST BATTERY

The battery used in this work is AGM Lead-Acid battery with nominal voltage of 12V and capacity of 100Ah. This battery's type is chosen because of its availability in our laboratory. While charged and in standby usage, the recommended voltage for individual cell is 2.28 V (6 cells in series). In addition, for cycle usage that requires fast charge, the maximum voltage is 2.45 V. Other characteristics of these batteries are shown in Table.4.

TABLE IV. 1ST BATTERY CHARACTERISTICS

Parameter	Value
Manufacturer	VISION
Model	6FM100E-X
Nominal capacity	100Ah
Nominal voltage	12V
Charging/discharging	Cut-off-voltage(13.8/10.8V)
Recommend charging current (0.25C)	25A
Maximum discharge current	(short time<5s) 900A
Design life	10 years
Operating temperature (charge/discharge)	-10C°-60C°/-20C°-60C°
Shell material	ABS
Weight	29Kg

✓ 2ND BATTERY

The battery used in this research is a valve regulated lead–acid (VRLA) battery with a nominal voltage of 12V and a capacity of 52Ah. The recommended voltage when charged for standby use is 1.75 V for a single cell (6 cells in series). Further features of this battery are shown in Table.5.

TABLE V. 2ND BATTERY CHARACTERISTICS

Cells Per Unit	6
Voltage Per Unit	12 V
Capacity	52 Ah @ 20hr-rate to 1.75V per cell @25°C (77°F)
Weight	Approx. 18 Kg (39.68 lbs.)
Maximum Discharge Current	500A(5sec)
Internal Resistance	Approx. 5.5 mΩ
Operating Temperature Range	Discharge: -15°C~50°C (5°F~122°F) Charge: -15°C~40°C (5°F~104°F) Storage: -15°C~40°C (5°F~104°F)
Float Charging Voltage	13.5 to 13.8 VDC/unit Average at 25°C (77°F)
Recommended Maximum Charging Current Limit	15.6A
Equalization and Cycle Service	14.4 to 15.0 VDC/unit Average at 25°C (77°F)
Self-Discharge	CSB Batteries can be stored for more than 6 months at 25°C (77°F).

B. *Measurement test bench*

✓ 1ST BATTERY

Fig.2.1st battery Test bench

1. Supply table
2. Lead-acid battery
3. Stabilized power supply
4. MultiMate
5. Current sensor
6. Variable resistor

✓ 2^{ND} BATTERY

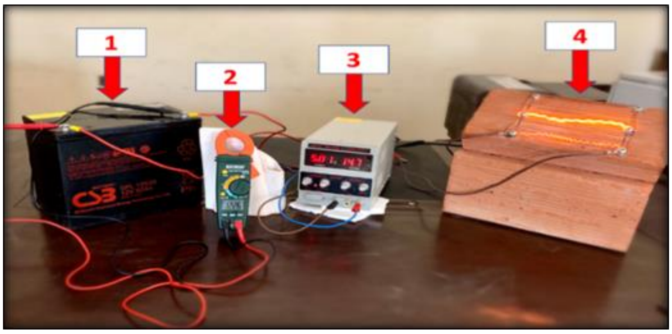

Fig.3. 2^{nd} Battery Test bench

1- A Lead Acid Battery
2- Clamp Meter
3- DC Power Supply
4- A Variable Resistor (Handmade)

C. Discharge process test

Two experiments are conducted for this test:

C1. Discharging with constant current (1st battery)

The variable resistor connected with the battery. Previously, the value of the resistor in discharge process is regulated at the value of the current of 10 A. The value of this resistor does not change in discharge process. Furthermore, the voltage and the current are measured every 5 min during the discharge process. After 10 hours and 17 minutes (37020 s), the value of cut-off voltage is achieved to 10.8 V. In this value, the variable resistor is disconnected. These tests were performed under an ambient temperature of 22° C.

C2. Discharging with variable C-rates current (2^{nd} battery)

the variable resistor is connected (to adjust it to a different C-rates discharge current 0.23C, 0.115C then 0.057C respectively. these values of C-rates in discharge current mode correspond to having three resistances connected in parallel. The value of each resistance is 3.225 Ω. During the first period, the discharge is done with 0.23C until 1.11 hours, at this time, the first resistance is disconnected, then the discharge continues with 0.115C until 4.44 hours, at this value the second resistance is disconnected. The discharge is pursued then with 0.057C until 7.23hours, at this time, the last resistance is disconnected and the experiment is stopped. The battery voltage and discharging current are measured each 5 minutes with a clamp meter during 7.23 hours. After 7.23 hours, the end of discharge is reached (cut-off voltage) which is equal to 10.39V. At this point, the discharge resistant is completely disconnected. The ambient temperature equals to T = 27.1 ° C.

IV. RESULTS AND DISCUSSION

A. 1st Battery

The simulations were performed with the following initial conditions of the discharge: SOC_0 =100 %, $Vdis_{int}$=12.6 V, $Vdis_{end}$=10.8 V and $Tdis_{sum}$=36000 s.

Fig.4. shows that the discharge voltage of the battery's datasheet and simulation are slightly different. This deference is due to the imprecision when extracting the parameters of battery model (Table.2) from the curve of the discharge voltage given by the manufacturer. The discharge voltage decreases to 10.8 V for 10 hours which is called the cut-off voltage. The value of 10.8 V does not correspond to the full discharge of battery (SOC = 0%) but is suitable to minimum SOC value which is equal to nearly 20% [113, 114].

Experimental discharge voltage is fitted to that of the simulation except that the value of the end of discharge voltage (10.8 V) is reached after a period of 10h and 17 minutes (37020 s). This difference indicates that the battery's capacity varies according to the parameters of exploitation (charge mode, the ambient temperature, the discharge current, the battery history ...etc.). Moreover, the voltage given by the manufacturer is related to ideal conditions (T = 25 C°, I_{dis}= 10 A, the battery State Of Health (SOH = 0%)). The three curves (datasheet, simulation and experimental) are superposed which indicate that the adopted model of the battery represents the actual behavior of the battery discharge phase with high accuracy.

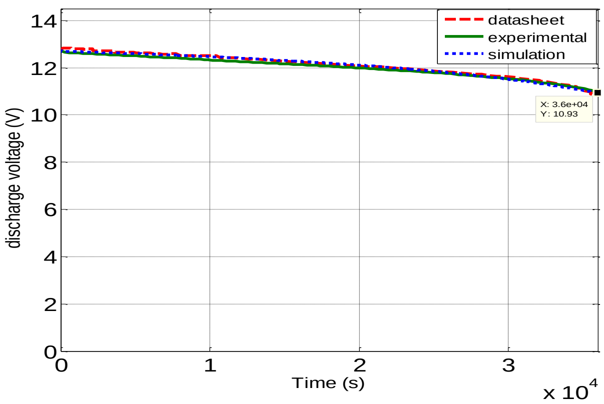

Fig.4.The discharge voltage versus time.

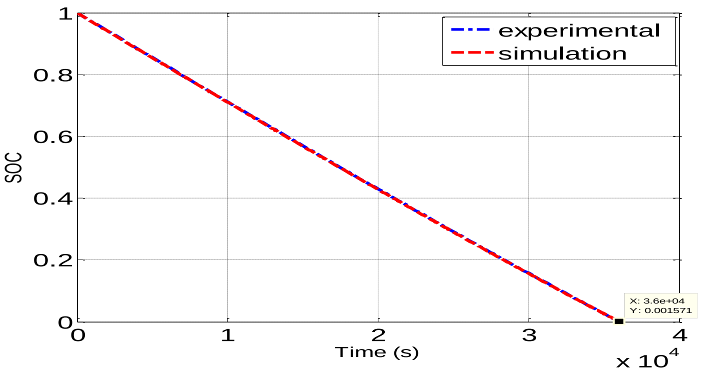

Fig.5.The state of charge (SOC) of the battery versus time

According to Fig.5, we note that the battery is initially full (SOC_0 = 100%) and after 10 hours the state of charge of the battery decreases to the minimum value (SOC_{min} = 20%). This value corresponds to the actual value of the Lead-Acid battery (SOC_{min} = 20%). [113, 115, 114, 108].

Furthermore, this value must not be exceeded in the aim to prevent the damage of the battery. The curve of the SOC estimated by the estimator of Coulomb Counting shows that the discharge of battery is under a constant discharge current (I_{dis}= 10 A). Although, this technique follows the state of charge of the battery throughout the discharge time (10 h). SOC_{exp} and SOC_{th} are fitted which indicate that this technique is very precise and robust.

B. 2nd Battery

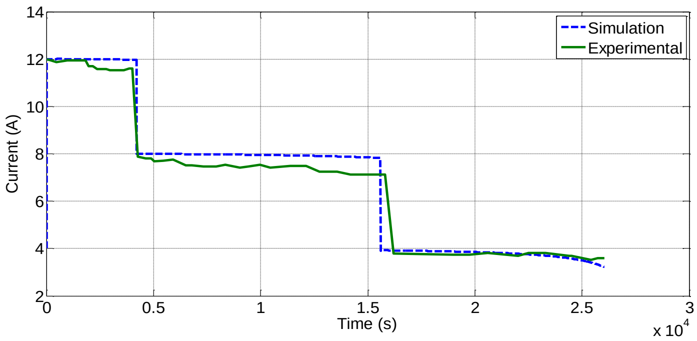

Fig.6. The discharge current as a function of time at different C-rates.

Figure.6 gives the result of the battery discharge using a handmade variable resistor (three equal resistors connected in parallel) where the total equivalent resistor equals to R_{eq1} = 1.075 ohms. At the beginning, all resistors are connected and a discharging rate of 0.23C is applied between [0 to 1.11 hours].Then, one resistance is disconnected from the total equivalent resistors to obtain R_{eq2} = 2.15 ohms, corresponding to a discharge rate of 0.115C between [1.11 to 4.44 hours]. Finally, a second resistance is disconnected, which means that only one resistance is kept connected, with a value of 3.225 ohms, corresponding to a a discharging rate at 0.057C between [4.44 to 7.23 hours].

Therefore, it is noticed that the current is constant during each C-rates of the discharging range. This is a safe and effective method. Where the minimum value of discharging current is 2.90 A, which corresponds to the value of the cutting voltage of 10.39V.

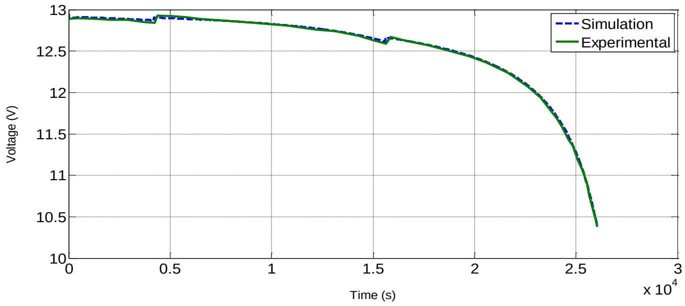

Fig.7. The discharge voltage as a function of time at different C-rates.

Figure.7 illustrates that with three ranges, the discharge voltage decreases to 10.39V for 7.23 hours.

From this curve, it can be noticed that these three ranges express the discharging with different C-rates, 0.23C, 0.115C, and 0.057C respectively.

The two curves (simulated and experimental) are almost the same; this shows that the generic battery presents the real behavior of the battery in the discharging process with a very high precision.

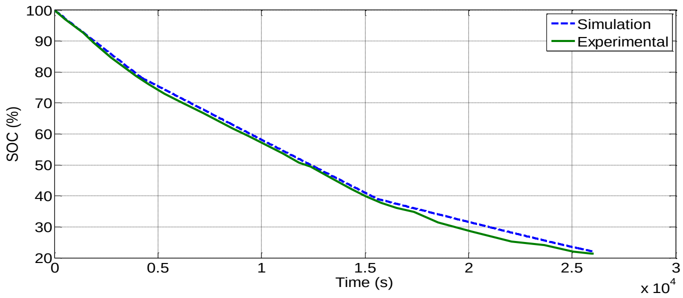

Fig.8. The SOC as a function of time at different C- rates.

The battery is initially fully charged (SOC_0 = 100%) according to figure 8, and the battery charging status decreases after 7.23 hours to the minimum value (SOC = 20%), corresponding to the recommended value of the lead-acid battery (SOC_{min} = 20%), this value must not be exceeded to prevent the battery from being harmed.

The SOC curve calculated by the coulomb counting estimator is a straight line, i.e., the discharge phase is performed under a different discharge current (I_{disch} = 12A, 6A then 3A, respectively), this technique followed well the state of charge the battery during the entire discharge period (7.23h).

$SOC_{experimental}$ and $SOC_{simulated}$ are almost the same, which shows that this technique is very accurate and usefull.

V. CONCLUSION

Based on the findings, it is evident that:

The discharging process exhibits high accuracy and favorable battery behavior under constant current conditions, particularly crucial for hybrid/electric vehicle applications.

The Ampere hour method proves highly precise in estimating battery state of charge across both constant and variable discharge currents, finding extensive use in embedded applications like hybrid/electric vehicles and renewable energy systems such as photovoltaic setups.

However, drawbacks include inherent inaccuracies and challenges in determining initial state of charge, necessitating the use of precise measurement instruments (voltage, current, temperature sensors) and periodic calibration.

Lead-acid batteries are primarily suited for short-distance vehicles, remaining the most cost-effective battery option per unit of stored energy and likely to maintain widespread usage in such applications. Many practical and industrial electric vehicles with shorter range requirements can be effectively manufactured.

The proposed method offers simplicity in implementation across portable devices and electric cars, requiring basic calculations and hardware specifications.

REFERENCES

[1] Hannan, M.A.; Hossain Lipu, M.S.; Hussain, A.; Mohamed, A. A review of lithium-ion battery state of charge estimation and management system in electric vehicle applications: Challenges and recommendations. Renew. Sustain. Energy Rev. 2017, 78, 834–854.

[2] Han, X.; Ouyang, M.; Lu, L.; Jianqiu, L. A comparative study of commercial lithium ion battery cycle life in electric vehicle: Capacity loss estimation. J. Power Sources 2014, 268, 658–669.

[3] Berecibar, M.; Gandiaga, I.; Villarreal, I.; Omar, N.; Van Mierlo, J.; Van den Bossche, P. Critical review of state of health estimation methods of Li-ion batteries for real applications. Renew. Sustain. Energy Rev. 2016, 56, 572–587.

[4] Rahman, M.A.; Anwar, S.; Izadian, A. Electrochemical model parameter identification of a lithium-ion battery using particle swarm optimization method. J. Power Sources 2016, 307, 86–97.

[5] Berecibar, M.; Gandiaga, I.; Villarreal, I.; Omar, N.; Van Mierlo, J.; Van den Bossche, P. Critical review of state of health estimation methods of Li-ion batteries for real applications. Renew. Sustain. Energy Rev. 2016, 56, 572–587.

[6] Zheng, Y.; Ouyang, M.; Han, X.; Lu, L.; Li, J. Investigating the error sources of the online state of charge estimation methods for lithium-ion batteries in electric vehicles. J. Power Sources 2018, 377, 161–188.

[7] Rahimi Eichi, H.; Ojha, U.; Baronti, F.; Chow, M.Y. Battery Management System: An Overview of Its Application in the Smart Grid and Electric Vehicles. IEEE Ind. Electron. Mag. 2013, 7, 4–16.

[8] Chen, K.; Sun, Y.; Li, T.; Sun, Z. Modeling and remaining capacity estimation of lithium-ion battery for electric vehicles. Qiche Gongcheng/Automotive Eng. 2014, 36, 404–408.

[9] Dong, B.; Tian, Y.; Zhou, C. One estimating method of the state of charge of power battery for electronic vehicle. In Proceedings of the 2014 Sixth International Conference on Measuring Technology and Mechatronics Automation, Zhangjiajie, China, 10–11 January 2014; pp. 439–442.

[10] Maltezo, M.R.C.; Thio-Ac, A.C.; Castillo, A.M.C.; Gattu, L.E.; Hernandez, C.E.A.; Labuan, J.J.C.; Navales, L.F.; Sopeña, E.C.; Arago, N.M.; Galido, E.A.; et al. Arduino-based battery monitoring system with state of charge and remaining useful time estimation. Int. J. Adv. Technol. Eng. Explor. 2021, 8, 432–444.

[11] Khan, M.A.A.; Khalid, H.A.; Balan, R.; Bakkaloglu, B. A novel State of Charge and State of Health estimation technique for Lithium-ion cells using machine learning based Pseudo-Random Binary Sequence method. J. Energy Storage 2022, 55, 105472.

[12] Hannan, M.A.; Hossain Lipu, M.S.; Hussain, A.; Mohamed, A. A review of lithium-ion battery state of charge estimation and management system in electric vehicle applications: Challenges and recommendations. Renew. Sustain. Energy Rev. 2017, 78, 834–854.

[13] Berecibar, M.; Gandiaga, I.; Villarreal, I.; Omar, N.; Van Mierlo, J.; Van den Bossche, P. Critical review of state of health estimation methods of Li-ion batteries for real applications. Renew. Sustain. Energy Rev. 2016, 56, 572–587.

[14] Zhang, J.; Zhang, L.; Li, Y.; Liu, H. The State-of-Charge Estimation of Supercapacitor With Kalman Filtering Algorithm. In Proceedings of the 2021 3rd International Conference on Electrical Engineering and Control Technologies (CEECT), Macau, China, 16–18 December 2021; pp. 208–211.

[15] Baba, A.; Adachi, S. SOC estimation of HEV/EV battery using series kalman filter. Electr. Eng. Jpn. 2014, 187, 53–62.

[16] Loukil, J.; Masmoudi, F.; Derbel, N. State of charge estimation of lead acid battery using a Kalman filter. In Proceedings of the 2017 14th International Multi-Conference on Systems, Signals & Devices (SSD), Marrakech, Morocco, 28–31 March 2017; pp. 308–312.

[17] Hattaha, K.; Ono, T.; Sasaki, R.; Osamura, K.; Adachi, S. State-of-Charge Estimation of Rechargeable Batteries guaranteed Finite-Time Estimation Error Convergence. In Proceedings of the 2019 SICE International Symposium on Control Systems (SICE ISCS), Kumamoto, Japan, 7–9 March 2019; pp. 72–77.

[18] Khan, H.F.; Hanif, A.; Ali, M.U.; Zafar, A. A Lagrange multiplier and sigma point Kalman filter based fused methodology for online state of charge estimation of lithium-ion batteries. J. Energy Storage 2021, 41, 102843.

[19] Wang, H.; Zheng, Y.; Yu, Y. Joint Estimation of SOC of Lithium Battery Based on Dual Kalman Filter. Processes 2021, 9, 1412.

[20] Sun, H.H.; Bi, J.; Shao, S. The state of charge estimation of lithium battery in electric vehicle based on extended kalman filter. Adv. Mater. Res. 2014, 953–954, 796–799.

[21] Yang, D.; Zhifu, W. BCRLS-EKF-based parameter identification and state-of-charge estimation approach of lithium-ion polymer battery in electric vehicles. In Society of Automotive Engineers (SAE)—China Congress; Springer: Singapore, 2018; p. 270.

[22] Huria, T.; Ludovici, G.; Lutzemberger, G. State of charge estimation of high power lithium iron phosphate cells. J. Power Sources 2014, 249, 92–102.

[23] Ramachandran, R.; Ganeshaperumal, D.; Subathra, B. Parameter Estimation of Battery Pack in EV using Extended Kalman Filters. In Proceedings of the 2019 IEEE International Conference on Clean Energy and Energy Efficient Electronics Circuit for Sustainable Development (INCCES), Krishnankoil, India, 18–20 December 2019; pp. 1–5.

[24] Yang, D.; Qi, G.; Li, X. State-of-charge estimation of LiFePO4/C battery based on extended Kalman filter. In Proceedings of the 2013 IEEE PES Asia-Pacific Power and Energy Engineering Conference (APPEEC), Hong Kong, China, 8–11 December 2013; pp. 1–5.

[25] Yang, D.; Liu, J.; Wang, Y.; Chen, M.; Zhang, B.; Li, Y. State-of-charge estimation using a self-adaptive noise extended Kalman filter for lithium batteries. In Proceedings of the 2014 IEEE PES Asia-Pacific Power and Energy Engineering Conference (APPEEC), Hong Kong, China, 7–10 December 2014; pp. 1–5.

[26] Ke, M.Y.; Chiu, Y.H.; Wu, C.Y. Battery Modelling and SOC Estimation of a LiFePO4 Battery. In Proceedings of the 2016 International Symposium on Computer, Consumer and Control (IS3C), Xi'an, China, 4–6 July 2016; pp. 208–211.

[27] Jarraya, I.; Masmoudi, F.; Chabchoub, M.H.; Trabelsi, H. An online state of charge estimation for Lithium-ion and supercapacitor in hybrid electric drive vehicle. J. Energy Storage 2019, 26, 100946.

[28] Ko, Y.; Choi, W. A New SOC Estimation for LFP Batteries: Application in a 10 Ah Cell (HW 38120 L/S) as a Hysteresis Case Study. Electronics 2021, 10, 705.

[29] Zheng, X.; Zhang, Z. State of charge estimation at different temperatures based on dynamic thermal model for lithium-ion batteries. J. Energy Storage 2022, 48, 104011.

[30] Seo, M.; Song, Y.; Kim, J.; Paek, S.W.; Kim, G.H.; Kim, S.W. Innovative lumped-battery model for state of charge estimation of lithium-ion batteries under various ambient temperatures. Energy 2021, 226, 120301.

[31] Wang, D.; Bao, Y.; Shi, J. Online Lithium-Ion Battery Internal Resistance Measurement Application in State-of-Charge Estimation Using the Extended Kalman Filter. Energies 2017, 10, 1284.

[32] Lin, L.; Fukui, M.; Takaba, K. An accurate SOC estimation system for lithium-ion batteries by EKF with dynamic noise adjustment. In Proceedings of the 2015 15th International Symposium on Communications and Information Technologies (ISCIT), Nara, Japan, 7–9 October 2015; pp. 33–36.

[33] Zhou, Z.; Duan, B.; Kang, Y.; Cui, N.; Shang, Y.; Zhang, C. A low-complexity state of charge estimation method for series-connected lithium-ion battery pack used in electric vehicles. J. Power Sources 2019, 441, 226972.

[34] Tudoroiu, R.E.; Zaheeruddin, M.; Radu, S.M.; Tudoroiu, N. Real-Time Implementation of an Extended Kalman Filter and a PI Observer for State Estimation of Rechargeable Li-Ion Batteries in Hybrid Electric Vehicle Applications—A Case Study. Batteries 2018, 4, 19.

[35] Jiang, N.; Pang, H. Study on Co-Estimation of SoC and SoH for Second-Use Lithium-Ion Power Batteries. Electronics 2022, 11, 1789.

[36] Chen, Z.; Li, X.; Shen, J.; Yan, W.; Xiao, R. A Novel State of Charge Estimation Algorithm for Lithium-Ion Battery Packs of Electric Vehicles. Energies 2016, 9, 710.

[37] Macicior, H.; Oyarbide, M.; Miguel, O.; Cantero, I.; Canales, J.M.; Etxeberria, A. Iterative capacity estimation of LiFePO4 cell over the lifecycle based on SoC estimation correction. World Electr. Veh. J. 2013, 6, 752–761.

[38] Xu, P.; Li, J.; Sun, C.; Yang, G.; Sun, F. Adaptive State-of-Charge Estimation for Lithium-Ion Batteries by Considering Capacity Degradation. Electronics 2021, 10, 122.

[39] Shen, X.; Shen, T.; Zha, X.; Hikiri, K. State-of-charge estimation of super-capacitor using dual extended Kalman filter. In Proceedings of the 33rd Chinese Control Conference, Nanjing, China, 28–30 July 2014; pp. 227–232.

[40] Wang, D.; Yang, Y.; Gu, T. A hierarchical adaptive extended Kalman filter algorithm for lithium-ion battery state of charge estimation. J. Energy Storage 2023, 62, 106831.

[41] Tran, N.T.; Khan, A.B.; Choi, W. State of Charge and State of Health Estimation of AGM VRLA Batteries by Employing a Dual Extended Kalman Filter and an ARX Model for Online Parameter Estimation. Energies 2017, 10, 137.

[42] Xiong, R.; Sun, F.C.; He, H.W. Data-driven State-of-Charge estimator for electric vehicles battery using robust extended Kalman filter. Int. J. Automot. Technol. 2014, 15, 89–96.

[43] Wu, M.; Qin, L.; Wu, G. State of charge estimation of Power lithium-ion battery based on an Affine Iterative Adaptive Extended Kalman Filter. J. Energy Storage 2022, 51, 104472.

[44] Su, J.; Schneider, S.; Yaz, E.; Josse, F. Online State of Charge Estimation of Lithium-ion Battery Cells: A Multiple Model Adaptive Estimation Approach. In Proceedings of the 2021 American Control Conference (ACC), New Orleans, LA, USA, 25–28 May 2021; pp. 4447–4452.

[45] Liu, X.; Li, K.; Wu, J.; He, Y.; Liu, X. An extended Kalman filter based data-driven method for state of charge estimation of Li-ion batteries. J. Energy Storage 2021, 40, 102655.

[46] Takyi-Aninakwa, P.; Wang, S.; Zhang, H.; Li, H.; Xu, W.; Fernandez, C. An optimized relevant long short-term memory-squared gain extended Kalman filter for the state of charge estimation of lithium-ion batteries. Energy 2022, 260, 125093.

[47] Wu, M.; Qin, L.; Wu, G. State of charge estimation of power lithium-ion battery based on an adaptive time scale dual extend Kalman filtering. J. Energy Storage 2021, 39, 102535.

[48] Wu, M.; Qin, L.; Wu, G.; Huang, Y.; Shi, C. State of Charge Estimation of Power Lithium-ion Battery Based on a Variable Forgetting Factor Adaptive Kalman Filter. J. Energy Storage 2021, 41, 102841.

[49] He, W.; Williard, N.; Chen, C.; Pecht, M. State of charge estimation for electric vehicle batteries using unscented kalman filtering. Microelectron. Reliab. 2013, 53, 840–847.

[50] Zheng, Y.; He, F.; Wang, W. A Method to Identify Lithium Battery Parameters and Estimate SOC Based on Different Temperatures and Driving Conditions. Electronics 2019, 8, 1391.

[51] Fu, S.; Lv, T.; Xie, J.; Wu, L.; Luo, C. A Multiple Time-Scales Based Multi-state Co-estimation Method for Lithium-ion Battery. In Proceedings of the 2021 11th International Conference on Power and Energy Systems (ICPES), Shanghai, China, 18–20 December 2021; pp. 183–189.

[52] Zeng, M.; Zhang, P.; Yang, Y.; Xie, C.; Shi, Y. SOC and SOH Joint Estimation of the Power Batteries Based on Fuzzy Unscented Kalman Filtering Algorithm. Energies 2019, 12, 3122.

[53] Yun, Z.; Qin, W.; Shi, W. State of charge estimation of lithium-ion battery under time-varying noise based on Variational Bayesian Estimation Methods. J. Energy Storage 2022, 52, 104916.

[54] Liu, S.; Cui, N.; Zhang, C. An Adaptive Square Root Unscented Kalman Filter Approach for State of Charge Estimation of Lithium-Ion Batteries. Energies 2017, 10, 1345.

[55] Lv, J.; Jiang, B.; Wang, X.; Liu, Y.; Fu, Y. Estimation of the State of Charge of Lithium Batteries Based on Adaptive Unscented Kalman Filter Algorithm. Electronics 2020, 9, 1425.

[56] Zheng, Q.; Yang, J.; Luo, Q.; Shi, K. Estimation of state of charge of lithium battery based on BCRLS-UKF algorithm. In Proceedings of the 2021 IEEE International Conference on Computer Science, Electronic Information Engineering and Intelligent Control Technology (CEI), Fuzhou, China, 24–26 September 2021; pp. 22–26.

[57] Miao, Y.; Gao, Z. Estimation for state of charge of lithium-ion batteries by adaptive fractional-order unscented Kalman filters. J. Energy Storage 2022, 51, 104396.

[58] Biswas, A.; Gu, R.; Kollmeyer, P.; Ahmed, R.; Emadi, A. Simultaneous State and Parameter Estimation of Li-Ion Battery with One State Hysteresis Model Using Augmented Unscented Kalman Filter. In Proceedings of the 2018 IEEE Transportation Electrification Conference and Expo (ITEC), Long Beach, CA, USA, 13–15 June 2018; pp. 1065–1070.

[59] Bhuvana, V.P.; Unterrieder, C.; Huemer, M. Battery Internal State Estimation: A Comparative Study of Non-Linear State Estimation Algorithms. In Proceedings of the 2013 IEEE Vehicle Power and Propulsion Conference (VPPC), Beijing, China, 15–18 October 2013; pp. 1–6.

[60] Linghu, J.; Kang, L.; Liu, M.; Luo, X.; Feng, Y.; Lu, C. Estimation for state-of-charge of lithium-ion battery based on an adaptive high-degree cubature Kalman filter. Energy 2019, 189, 116204.

[61] Chen, X.; Shen, W.; Cao, Z.; Kapoor, A. Adaptive gain sliding mode observer for state of charge estimation based on combined battery equivalent circuit model in electric vehicles. In Proceedings of the 2013 IEEE 8th Conference on Industrial Electronics and Applications (ICIEA) Melbourne, VIC, Australia, 19–21 June 2013; pp. 601–606.

[62] Xia, B.; Chen, C.; Tian, Y.; Sun, W.; Xu, Z.; Zheng, W. A novel method for state of charge estimation of lithium-ion batteries using a nonlinear observer. J. Power Sources 2014, 270, 359–366.

[63] Othman, B.M.; Salam, Z.; Husain, A.R. A computationally efficient adaptive online state-of-charge observer for Lithium-ion battery for electric vehicle. J. Energy Storage 2022, 49, 104141.

[64] Brembeck, J. A Physical Model-Based Observer Framework for Nonlinear Constrained State Estimation Applied to Battery State Estimation. Sensors 2019, 19, 4402.

[65] Tran, N.T.; Khan, A.B.; Nguyen, T.T.; Kim, D.W.; Choi, W. SOC Estimation of Multiple Lithium-Ion Battery Cells in a Module Using a Nonlinear State Observer and Online Parameter Estimation. Energies 2018, 11, 1620.

[66] Guoliang, W.; Rengui, L.; Chunbo, Z.; Chan, C. State of charge Estimation for NiMH Battery based on electromotive force method. In Proceedings of the 2008 IEEE Vehicle Power and Propulsion Conference, Harbin, China, 3–5 September 2008; pp. 1–5.

[67] Siqueira, H.; Macedo, M.; Tadano, Y.d.S.; Alves, T.A.; Stevan, S.L., Jr.; Oliveira, D.S., Jr.; Marinho, M.H.; Neto, P.S.d.M.; Oliveira, J.F.d.; Luna, I.; et al. Selection of temporal lags for predicting riverflow series from hydroelectric plants using variable selection methods. Energies 2020, 13, 4236.

[68] Belotti, J.; Siqueira, H.; Araujo, L.; Stevan, S.L., Jr.; de Mattos Neto, P.S.; Marinho, M.H.; de Oliveira, J.F.L.; Usberti, F.; Leone Filho, M.d.A.; Converti, A.; et al. Neural-based ensembles and unorganized machines to predict streamflow series from hydroelectric plants. Energies 2020, 13, 4769.

[69] Kang, L.; Zhao, X.; Ma, J. A new neural network model for the state-of-charge estimation in the battery degradation process. Appl. Energy 2014, 121, 20–27.

[70] Gao, A.Y.; Zhang, F.L.; Fu, Z.M.; Zhang, Z.C.; Li, H.D. The SOC estimation and simulation of power battery based on self-recurrent wavelet neural network. In Proceedings of the 2017 Chinese Automation Congress (CAC), Jinan, China, 20–22 October 2017; pp. 4247–4252.

[71] Zhang, C.W.; Chen, S.R.; Gao, H.B.; Xu, K.J.; Yang, M.Y. State of Charge Estimation of Power Battery Using Improved Back Propagation Neural Network. Batteries 2018, 4, 69.

[72] Bezha, M.; Nagaoka, N. Online learning ANN model for SoC estimation of the Lithium- Ion battery in case of small amount of data for practical applications. In Proceedings of the 2019 10th International Conference on Power Electronics and ECCE Asia (ICPE 2019—ECCE Asia), Busan, Republic of Korea, 27–30 May 2019; pp. 1–5.

[73] de Mattos Neto, P.S.; de Oliveira, J.F.L.; Júnior, D.S.d.O.S.; Siqueira, H.V.; Marinho, M.H.D.N.; Madeiro, F. A hybrid nonlinear combination system for monthly wind speed forecasting. IEEE Access 2020, 8, 191365–191377.

[74] Gu, T.; Wang, D. A beetle antennae search optimized recurrent extreme learning machine for battery state of charge estimation. Energy Res. 2022, 46, 19190–19205.

[75] Ströbel, M.; Pross-Brakhage, J.; Kopp, M.; Birke, K.P. Impedance Based Temperature Estimation of Lithium Ion Cells Using Artificial Neural Networks. Batteries 2021, 7, 85.

[76] Ezemobi, E.; Silvagni, M.; Mozaffari, A.; Tonoli, A.; Khajepour, A. State of Health Estimation of Lithium-Ion Batteries in Electric Vehicles under Dynamic Load Conditions. Energies 2022, 15, 1234.

[77] Hamida, M.A.; El-Sehiemy, R.A.; Ginidi, A.R.; Elattar, E.; Shaheen, A.M. Parameter identification and state of charge estimation of Li-Ion batteries used in electric vehicles using artificial hummingbird optimizer. J. Energy Storage 2022, 51, 104535.

[78] Bonfitto, A.; Feraco, S.; Tonoli, A.; Amati, N.; Monti, F. Estimation Accuracy and Computational Cost Analysis of Artificial Neural Networks for State of Charge Estimation in Lithium Batteries. Batteries 2019, 5, 47.

[79] Bonfitto, A. A Method for the Combined Estimation of Battery State of Charge and State of Health Based on Artificial Neural Networks. Energies 2020, 13, 2548.

[80] Lipu, M.S.H.; Hannan, M.A.; Hussain, A.; Ayob, A.; Saad, M.H.M.; Muttaqi, K.M. State of Charge Estimation in Lithium-Ion Batteries: A Neural Network Optimization Approach. Electronics 2020, 9, 1546.

[81] Park, J.; Lee, J.; Kim, S.; Lee, I. Real-Time State of Charge Estimation for Each Cell of Lithium Battery Pack Using Neural Networks. Appl. Sci. 2020, 10, 8644.

[82] Lee, J.H.; Lee, I.S. Lithium Battery SOH Monitoring and an SOC Estimation Algorithm Based on the SOH Result. Energies 2021, 14, 4506.

[83] Lee, J.H.; Lee, I.S. Estimation of Online State of Charge and State of Health Based on Neural Network Model Banks Using Lithium Batteries. Sensors 2022, 22, 5536.

[84] Cui, Z.; Kang, L.; Li, L.; Wang, L.; Wang, K. A hybrid neural network model with improved input for state of charge estimation of lithium-ion battery at low temperatures. Renew. Energy 2022, 198, 1328–1340.

[85] Mendes, J.; Araújo, R.; Sousa, P.; Apóstolo, F.; Alves, L. An architecture for adaptive fuzzy control in industrial environments. Comput. Ind. 2011, 62, 364–373.

[86] Shafiekhani, A.; Mahjoob, M.; Akraminia, M. Design and implementation of an adaptive critic-based neuro-fuzzy controller on an unmanned bicycle. Mechatronics 2015, 28, 115–123.

[87] Öztürk, N.; Çelik, E. Speed control of permanent magnet synchronous motors using fuzzy controller based on genetic algorithms. Int. J. Electr. Power Energy Syst. 2012, 43, 889–898.

[88] Hou, S.; Qian, Y.; Zhang, Z.; Han, J. Neural Networks for State-of-Charge Estimation of Li-ion Batteries. In Proceedings of the 2021 18th

International Conference on Electrical Engineering/Electronics, Computer, Telecommunications and Information Technology (ECTI-CON), Chiang Mai, Thailand, 19–22 May 2021; pp. 729–732.

[89] Gruosso, G.; Gajani, G.S.; Ruiz, F.; Valladolid, J.D.; Patino, D. A Virtual Sensor for Electric Vehicles' State of Charge Estimation. Electronics 2020, 9, 278.

[90] Surya, S.; Saldanha, C.C.; Williamson, S. Novel Technique for Estimation of Cell Parameters Using MATLAB/Simulink. Electronics 2022, 11, 117.

[91] Jafari, S.; Shahbazi, Z.; Byun, Y.C. Lithium-Ion Battery Health Prediction on Hybrid Vehicles Using Machine Learning Approach. Energies 2022, 15, 4753.

[92] Jafari, S.; Shahbazi, Z.; Byun, Y.C.; Lee, S.J. Lithium-Ion Battery Estimation in Online Framework Using Extreme Gradient Boosting Machine Learning Approach. Mathematics 2022, 10, 888.

[93] Li, X.; Wang, Z.; Zhang, L. Co-estimation of capacity and state-of-charge for lithium-ion batteries in electric vehicles. Energy 2019, 174, 33–44.

[94] Shen, H.; Zhou, X.; Wang, Z.; Wang, J. State of charge estimation for lithium-ion battery using Transformer with immersion and invariance adaptive observer. J. Energy Storage 2022, 45, 103768.

[95] Zhang, X.; Zhang, R. Estimation of Lithium Battery SOC Based on Fuzzy Unscented Kalman Filter Algorithm. In Proceedings of the 2021 IEEE/IAS Industrial and Commercial Power System Asia (I&CPS Asia), Chengdu, China, 18–21 July 2021; pp. 200–204.

[96] He, W.; Williard, N.; Chen, C.; Pecht, M. State of charge estimation for Li-ion batteries using neural network modeling and unscented Kalman filter-based error cancellation. Int. J. Electr. Power Energy Syst. 2014, 62, 783–791.

[97] Zahid, T.; Xu, K.; Li, W.; Li, C.; Li, H. State of charge estimation for electric vehicle power battery using advanced machine learning algorithm under diversified drive cycles. Energy 2018, 162, 871–882.

[98] Rahbari, O.; Omar, N.; Firouz, Y.; Rosen, M.A.; Goutam, S.; Bossche, P.V.D.; Mierlo, J.V. A novel state of charge and capacity estimation technique for electric vehicles connected to a smart grid based on inverse theory and a metaheuristic algorithm. Energy 2018, 155, 1047–1058.

[99] Shen, J.; Wang, Q.; Zhao, G.; Ma, Z.; He, Y. A joint moving horizon strategy for state-of-charge estimation of lithium-ion batteries under combined measurement uncertainty. J. Energy Storage 2021, 44, 103316

[100] Poloei, F.; Akbari, A.; Liu, Y.F. A Moving Window Least Mean Square Approach to State of Charge Estimation for Lithium Ion Batteries. In Proceedings of the 2019 1st Global Power, Energy and Communication Conference (GPECOM), Nevsehir, Turkey, 12–15 June 2019; pp. 398–402.

[101] Arasaratnam, I.; Tjong, J.; Ahmed, R. Battery management system in the Bayesian paradigm: Part I: SOC estimation. In Proceedings of the 2014 IEEE Transportation Electrification Conference and Expo (ITEC), Dearborn, MI, USA, 15–18 June 2014; pp. 1–5.

[102] Lin, Q.; Wang, J.; Xiong, R.; Shen, W.; He, H. Towards a smarter battery management system: A critical review on optimal charging methods of lithium ion batteries. Energy 2019, 183, 220–234.

[103] W. Junping, C. Quanshi, and C. Binggang, "Support vector machine based battery model for electric vehicles," Energy Convers. Manag., vol. 47, no. 7–8, pp. 858–864, May 2006.

[104] F. Feng, R. Lu, and C. Zhu, "A Combined State of Charge Estimation Method for Lithium-Ion Batteries Used in a Wide Ambient Temperature Range," Energies 2014, Vol. 7, Pages 3004-3032, vol. 7, no. 5, pp. 3004–3032, May 2014.

[105] S. Zhang, X. Guo, X. Dou, and X. Zhang, "A data-driven coulomb counting method for state of charge calibration and estimation of lithium-ion battery," Sustain. Energy Technol. Assessments, vol. 40, p. 100752, Aug. 2020.

[106] A. Gismero, E. Schaltz, and D. I. Stroe, "Recursive State of Charge and State of Health Estimation Method for Lithium-Ion Batteries Based on Coulomb Counting and Open Circuit Voltage," Energies 2020, Vol. 13, Page 1811, vol. 13, no. 7, p. 1811, Apr. 2020.

[107] H. Hinz, "Comparison of Lithium-Ion Battery Models for Simulating Storage Systems in Distributed Power Generation," Invent. 2019, Vol. 4, Page 41, vol. 4, no. 3, p. 41, Aug. 2019.

[108] "Battery Management Systems," Batter. Manag. Syst., 2008.

[109] O. Tremblay, L. A. Dessaint, and A. I. Dekkiche, "A generic battery model for the dynamic simulation of hybrid electric vehicles," VPPC 2007 - Proc. 2007 IEEE Veh. Power Propuls. Conf., pp. 284–289, 2007.

[110] K. S. Ng, C. S. Moo, Y. P. Chen, and Y. C. Hsieh, "Enhanced coulomb counting method for estimating state-of-charge and state-of-health of lithium-ion batteries," Appl. Energy, vol. 86, no. 9, pp. 1506–1511, Sep. 2009.

[111] B. Zine, K. Marouani, M. Becherif, and S. Yahmedi, "Estimation of Battery Soc for Hybrid Electric Vehicle using Coulomb Counting Method," Int. J. Emerg. Electr. Power Syst., vol. 19, no. 2, Apr. 2018.

[112] R. Baroody, "UNLV Theses, Dissertations, Professional Papers, and Capstones," 2009.

[113] R. Yang, R. Xiong, H. He, and Z. Chen, "A fractional-order model-based battery external short circuit fault diagnosis approach for all-climate electric vehicles application," J. Clean. Prod., vol. 187, pp. 950–959, Jun. 2018.

[114] Z. Wang, J. Xu, and T. Wang, "The online monitoring system software design and the SOC estimation algorithm research for power battery," Proc. 2013 IEEE Int. Conf. Veh. Electron. Safety, ICVES 2013, pp. 89–92, 2013.

[115] C. Weng, J. Sun, and H. Peng, "A unified open-circuit-voltage model of lithium-ion batteries for state-of-charge estimation and state-of-health monitoring," J. Power Sources, vol. 258, pp. 228–237, Jul. 2014.